Enhancement of the Mechanical Properties of Directly Spun CNT Fibers by Chemical Treatment

Slawomir Boncel, Rajyashree M. Sundaram, Alan H. Windle, and Krzysztof K. K. Koziol*

Department of Materials Science and Metallurgy, University of Cambridge, Pembroke Street, Cambridge CB2 3QZ, United Kingdom

ABSTRACT

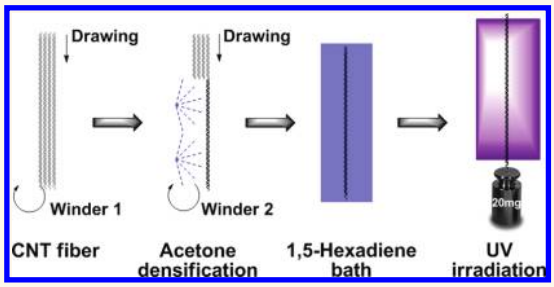

Translating the remarkable mechanical properties of individual carbon nanotubes to macroscopic assemblies presents a unique challenge in maximizing the potential of these remarkable entities for new materials. Infinitely long individual nanotubes would represent the ideal molecular building blocks; however, in the case of length-limited nanotubes, typically in the range of micro- and millimeters, an alternative strategy could be based on the improvement of the mechanical coherency between bundles assembling the macroscopic materials, like fibers or films. Here, we present a method to enhance the mechanical performance of fibers continuously spun from a CVD reactor, by a postproduction processing methodology utilizing a chemical agent aided by UV irradiation. The treatment results in an increase of 100% in specific strength and 300% in toughness of the fibers with strength values rocketing to as high as 3.5 GPa SG^{-1}. An attempt has been made to explore the nature of the chemical modifications introduced in the fiber and the consequential effects on its properties.

KEYWORDS: carbon nanotube fibers · carbon nanotube yarns · mechanical properties · chemical cross-linking

Fundamental research on carbon nanotubes (CNTs) and CNT-based materials is eliciting intense interest from the scientific research community. Due to their excellent mechanical properties, as well as superior electrical and thermal conductivities,[1,2] carbon nanotubes show promise for multifunctional materials for a range of applications. Nevertheless, the transfer of the science into a realistic technology has yet to be completed, and key challenges remain, especially in terms of self-assembling the nanotubes to form useful materials on a macroscopic scale which express the exciting properties of their nanotube building blocks.[3] Substantial attention is required toward the control of interaction between nanotubes, which plays a major role in load transfer[4] and electron[5] and phonon transport.[6] The direct assembly of CNTs into fibers involving continuous spinning from a chemical vapor deposition (CVD) reactor[7,8] is a significant step toward the scalable production of macroscopic entities of CNTs. This process, at the laboratory scale, can generate kilometers of ~10 μm diameter fiber, consisting of millimeter-long collapsed double-walled nanotubes (d = 5–10 nm), arranged into bundles (Figure 1). The CNT fiber shows, on a macroscale, attractive mechanical properties[8–10] but only a fraction of those reported for individual nanotubes. Nevertheless, the CNT fiber is already in the high-performance materials range.[11–14] The sliding of bundles (as shown in Figure 1C,D) of CNTs past each other (graphite is a lubricant) during stress transfer is the major limiting factor of the mechanical properties of the fiber under tensile loading.[15,16]

Of the various methods for making carbon nanotube fibers reported,[17–19] those produced by the coagulation method,[17] where the nanotube fiber is spun in a polymeric matrix, point to several advantages resulting from the presence of the polymer, especially with regard to strain to failure and energy absorbed before tensile failure.

The preferentially aligned macroscopic assemblies of carbon nanotubes were synthesized using the direct spinning CVD method.[7] The synthesis process operates in the temperature range of 1100–1400 °C. Ferrocene is used as the source of iron catalyst, thiophene is used as the source of sulfur for catalyst activation, and different carbon supply is used for supplying the main building element of the nanotubes. CNTs are rapidly synthesized in the hot zone with residence time not exceeding 10 s. The network of

* Address correspondence to kk292@cam.ac.uk.

Received for review August 28, 2010 and accepted November 20, 2011.

Published online November 21, 2011
10.1021/nn202685x

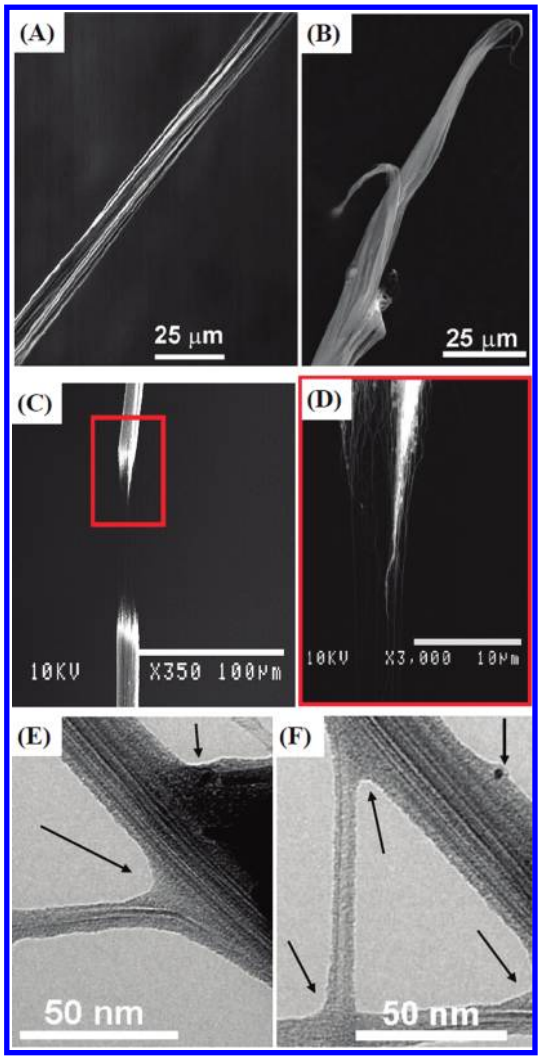

Figure 1. (A) Electron microscopy image of as-produced CNT fiber, using CVD reactor, (B) fracture surface of the as-made fiber with typical pull out fracture mechanism, (C,D) CNT fiber undergoing fracture with long bundles bridging the fiber ends. (E,F) Transmission electron microscope images with representative bundles, components of the fiber, and the extraneous surface coating (highlighted by the black arrows).

nanotubes is then continuously spun from one side of the open reactor into uniform fibers of around 10 μm in diameter using a condensation process.[8] The condensation of the fiber is achieved by spraying acetone onto the extracted assemblies of the nanotubes. The densified fiber is described here as as-made. The CNT fibers have large accessible surface area (~400 m^2 g^{-1} measured using the BET method), as shown by its ability to adsorb gaseous and liquid species. The rationale adopted in this work was to back diffuse a liquid monomeric species into the fiber and to initiate polymerization with UV radiation. The monomer chosen here was an α,ω-alkadiene, 1,5-hexadiene (HDE), which has a low viscosity[20] and is widely available.[21−23] The process for producing the treated fiber is summarized in Figure 2.

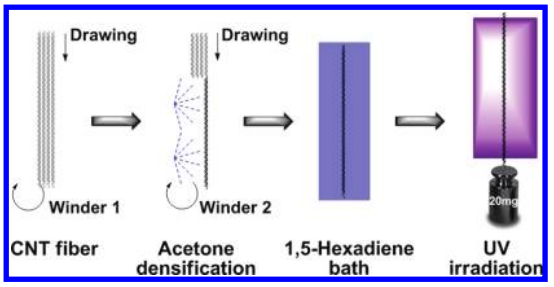

Figure 2. Process for chemical treatment of CNT fibers. Initially the CNT fiber is densified by acetone vapor and subjected to immersion in a bath containing HDE followed by UV irradiation. The fiber is maintained under a small tension (with a weight of 20 mg attached to the end of the fiber in order to reduce a distance between bundle coatings) during irradiation.

RESULTS

The as-drawn densified fibers (the production of which is described elsewhere[8]) were immersed in a bath containing 1,5-HDE (Acros Organics, >95%) for 5 min and subsequently exposed to UV radiation (λ = 254 nm, power = 8 W) for various time intervals (Figure 2). In addition, as controls, the fibers were irradiated in the absence of the external agent in order to estimate the effect of solely the radiation, while the effect of the HDE without subsequent UV radiation was also assessed.

Measurements of fiber properties for the different treatments are given in Figure 3. The height of the bars corresponds to the average value of the property over several samples. The standard deviation range is also indicated as the highest value recorded in each case (represented by circles).

Focusing first on the data for specific strength (Figure 3A), it is apparent that the immersion in HDE produces a reduction in specific strength by ~35%. We assign this reduction in significant part to the increase in weight of the fiber (~23%) associated with the adsorbed liquid which remains in the fiber after removal from the HDE bath. The values of mass changes obtained from the microbalance measurements for the as-drawn and treated fibers are shown in Table S1 in the Supporting Information. Turning to the effect of UV on the fiber without added HDE, there is no change in specific strength within the statistical deviation, although, nor any change in the fiber weight. The increase in specific strength on cross-linking, especially at the optimum UV exposure of 30 min, is, however, very significant, with the mean values being nearly doubled from 1.25 to 2.3 GPa SG^{-1}, with a high value of 3.5 GPa SG^{-1} observed for one sample. The mass increase as a result of the adsorbed HDE is reduced to only 8% after the UV treatment, a fact which we assign to the loss of further non-cross-linked material due to the temperature increase during UV treatment, which was measured to be ~40 °C (bp of HDE = 59.5 °C[24]).

Interestingly, 1,5-hexadiene was shown to photopolymerize and cross-link within 30 min to a final conversion

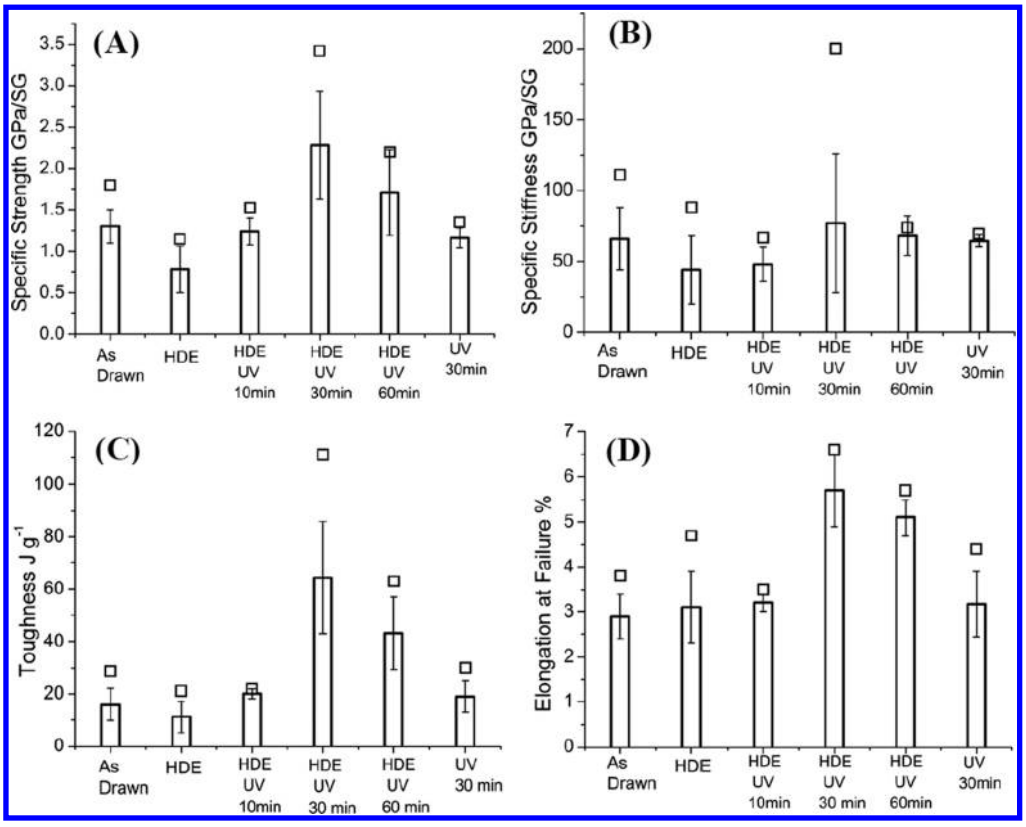

Figure 3. Comparison of the average (A) specific strength, (B) stiffness, (C) toughness, and (D) elongation at failure of fibers as-drawn and those immersed in HDE followed by exposure to UV radiation for 0 (HDE), 10 (HDE UV 10 min), 30 (HDE UV 30 min), and 60 (HDE UV 60 min) min, in addition to UV radiation for 30 min without immersion in HDE (UV 30 min). The error bars represent the standard deviation in the values. The squares are the maximum values measured.

of 87%,[21] which appears to match our optimum time scale of the chemical treatment.

Figure 3B–D shows the effect of the different treatments on other mechanical properties of the fiber samples: elastic stiffness, toughness (energy absorbed up until fracture (J g^{-1})), and strain to failure. The treatment which so dramatically increases the strength has virtually no effect on the stiffness of the fiber (except one measurement of 200 N tex^{-1} for one sample tested after UV treatment for 30 min). The elongation to failure is like the strength considerably increased, and as a result so is the toughness, in this case from 17 to 63 J g^{-1}. These data are obviously interrelated, and their association is clear from the stress/strain curves reproduced in Figure 4. It is interesting that for the curve from the optimum treatment (30 min UV) the specific stress/strain curve appears to steepen slightly beyond the point where an untreated fiber would fracture (3%) before its extension to some 6% before final fracture.

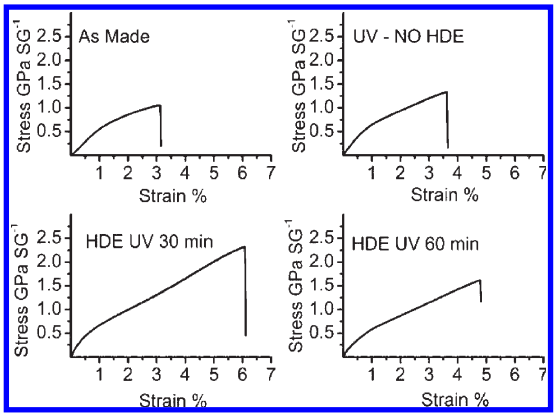

Figure 4. Typical tensile behavior of the as-made, UV-treated (in the absence of prior immersion in HDE), and HDE-UV-treated (30 and 60 min UV exposures) fibers.

DISCUSSION

Mechanical Data. The fact that the HDE-UV treatment radically improves the strength, elongation, and toughness of the fiber without having significant effect on the stiffness suggests that it is affecting some type of defect-based fracture mechanism previously proposed.[8] Microscopy of the fiber fracture mechanism itself indicates that this is due to the breakdown of the network of nanotube bundles, causing them to slide past each other. It would appear therefore that the cross-linked HDE is enhancing the bundle interconnectivity and increasing the mechanical performance of the network. The orientation of the nanotubes with the fiber axis has been shown to be of a high order,[25] and thus the reason why the elastic modulus is so much less than the theoretical in-plane value for a graphene layer (only ~10% of it) must be either associated with the

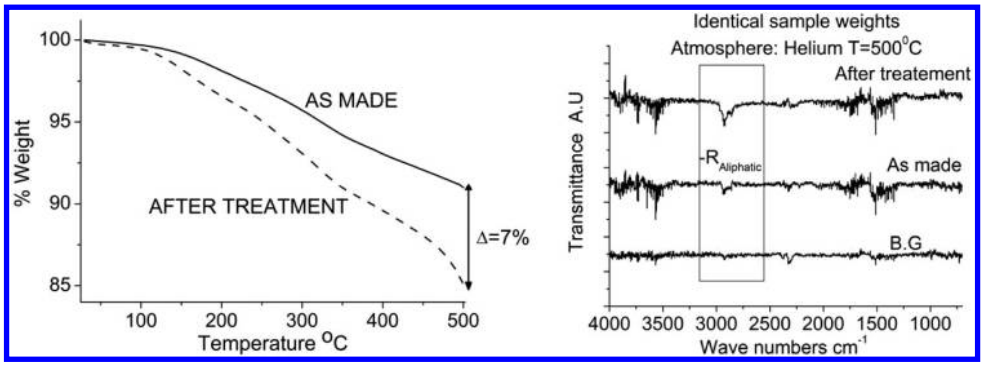

Figure 5. Thermograms of the as-made and the HDE-UV-treated fibers (left); IR spectra of gaseous products evolved during the TGA at 500 °C of the as-made and the HDE-UV-treated samples. The background (BG) spectrum is also shown (right).

transfer of stress from one nanotube to its neighbor within a bundle or the consequence of some sliding mechanism at the interbundle network points. However, a treatment which does not apparently penetrate the bundles, but is involved more with interbundle connectivity, would be expected to influence stiffness in some measure. The unusual, yet definite, increase in the slope of the stress−strain curve around 3% elongation may be significant here, as a cross-linking mechanism between the bundles which itself has extensibility, such as provided by say, a polymeric material, may be expected to show these characteristics.

Evidence for the Role of Extraneous Material as Impurities in the As-Spun Fiber. Returning briefly to Figure 1E,F, closer inspection of the image shows that the bundles are coated with a thin layer of nongraphitic material, and where two bundles are in contact, as in this particular case, the surface material can be seen forming a concave meniscus between them. Further evidence for the presence of this material comes from thermal gravimetric studies of the fiber. There is an evident weight loss on heating in the temperature region where decomposition of an amorphous/polymeric material is expected, while simultaneous IR spectroscopy clearly suggests that the material is chemically different from graphite or nanotubes (Figure 5).

It appears that this additional material or its decomposition products can be driven off the fiber thermally. The application of HDE-UV treatment to annealed fibers results in no significant change in the mechanical properties. We are therefore tempted to deduce that the extraneous material is needed to achieve a strength increase using HDE-UV, and that it may itself play some role in contributing to the mechanical integrity of the network. In addition, the optimum treatment was repeated but with toluene to assess the important role of HDE as an active agent. In this case, there was no detectable effect of the treatment on the strength, the stiffness, the elongation to fracture, or the energy absorbed. Hence, it is the cross-linking ability of the added liquid (HDE) which is key to its role in fiber strengthening.

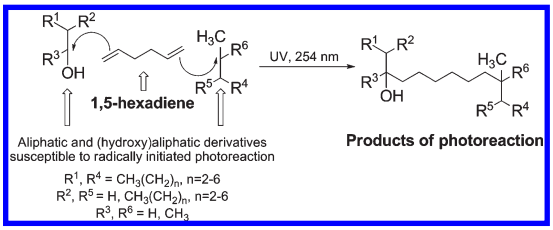

Scheme 1. Photoinitiated, free-radical chemical modification of the main components in the indigenous CNT fiber with 1,5-hexadiene molecules indicating the most susceptible reaction centers.

The next question is what the structure of this extraneous carbonaceous material is and the most probable mechanism for the HDE-UV cross-linking. The material was extracted from the fiber using prolonged immersion in solvents such as acetone, toluene, and $CDCl_3$, and the results of a combined FT-IR, $^1H/^{13}C$ NMR, and GC-MS analysis (Figures S1−S5) showed that it was essentially a mixture of aliphatic oligomers bearing a proportion of hydroxy groups. Ethanol pyrolysis studies in the literature often report[26−28] the formation of an oligo- and polymeric, mostly aliphatic, resinous material as a product of a minor radical reaction involving self-condensation of ethanol (and acetaldehyde formed as a product of thermolysis of ethanol). The presence of such coatings on nanotube bundles, but not on the surfaces of the individual nanotubes within the bundles, is becoming increasingly noticeable on micrographs (which is often disregarded being extraneous) as an intrinsic product of the CVD reaction where ethanol or other alcohols are used as the feedstock. It appears that the specific nature of the extraneous material is important in enabling the HDE-UV product to enhance interbundle connectivity, possibly by acting as a linking agent which will form covalent bonds with the activated double bonds at either end of the HDE molecule as envisaged in Scheme 1.

Apart from the aliphatic and hydroxyaliphatic compounds, other species present in the extraneous material, in much lower concentration, including esters or alkylaromatics can serve as reaction centers due to their enhanced stability by resonance of α-carbonyl and

benzyl radicals, respectively. It is rather unlikely that the surfaces of pristine nanotubes would provide the necessary active centers for this reaction, for they are expected to offer a much higher chemical stability than amorphous materials due to the low density of defects and dangling bonds.[29,30] In addition, the possibility of pristine CNTs themselves being reaction centers is remote, in the presence of species of higher reactivities, although under certain conditions, interactions between single-walled CNTs and alkenes are known and explored.[31,32]

CONCLUSIONS

In the pursuit for high-performance carbon-nanotube-based fibers, we have developed and optimized a simple, promising, and effective postsynthesis protocol for enhancing the fiber strength, elongation to fracture, and toughness by using 1,5-HDE infiltration followed by UV-initiated photopolymerization. It is predicted that extraneous resinous carbonaceous material, specifically of aliphatic nature, produced as a byproduct of the fiber synthesis in the CVD reactor, which coats the bundles, acts as anchoring points for the external reagent molecules. The process resulted in a dramatic improvement in the mechanical properties of the CNT fiber, that is, an increase of 100% in specific strength and 300% in toughness, but with no significant increase in stiffness. In this context, the increase in strength coupled with little increase in stiffness commends it to applications such as body armor where the figure of merit for a fiber is $\sigma' E' \varepsilon_F$, where σ' is the specific strength, E' the specific stiffness, and ε_F the strain to fracture. The fact that a single fiber treatment nearly quadruples the figure of merit by approximately doubling both the strength and the strain to fracture is an important move in the right direction.

METHODS

The tensile behavior of the treated fibers was studied using a dedicated machine (Textechno Favimat), with a 0−2 N load cell with a resolution 10^{-6} N. A standard gauge length of 20 mm and an elongation rate of 2 mm min^{-1} were used for all of the tests, with the machine also giving readings for linear density *via* mechanical resonance measurements, enabling the data to be plotted as specific strength and specific stiffness (expressed in N tex^{-1}, which is numerically equivalent to GPa SG^{-1}, where tex = g km^{-1} and SG is specific gravity). Additionally, mass changes after the immersion of the fiber in HDE and its subsequent UV treatment were followed using an ultramicrobalance (Sartorius, detection limit = 0.0001 mg).

Acknowledgment. The authors thank A. Gumrah Dumanli, R. Stearn, and W. Hough for stimulating discussions. R.M.S. would like to thank the Cambridge Commonwealth Trust for graduate student scholarship. K.K.K.K. thanks The Royal Society for funding.

Supporting Information Available: Additional experimental details. This material is available free of charge *via* the Internet at http://pubs.acs.org.

REFERENCES AND NOTES

1. Saito, R.; Dresselhaus, M. S.; Dresselhaus, G. *Physical Properties of Carbon Nanotubes*; Imperial College Press: London, 1998.
2. Dresselhaus, M. S.; Dresselhaus, G. *The Science of Fullerenes and Carbon Nanotubes: Their Properties and Applications*; Academic Press: New York, 1996.
3. Wang, X.; Li, Q.; Xie, J.; Jin, Z.; Wang, J.; Li, Y.; Jiang, K.; Fan, S. Fabrication of Ultralong and Electrically Uniform Single-Walled Carbon Nanotubes on Clean Substrates. *Nano Lett.* **2009**, *9*, 3137–3141.
4. Tsai, J.; Lu, T. Investigating the Load Transfer Efficiency in Carbon Nanotubes Reinforced Nanocomposites. *Compos. Struct.* **2009**, *2*, 172–179.
5. Vichchulada, P.; Vairavapandian, D.; Lay, M. D. Device Structures Composed of Single-Walled Carbon Nanotubes. *Nanoscience and Nanotechnology for Chemical and Biological Defense*; American Chemical Society: Washington, DC, 2009; Vol. 1016, pp 59−72.
6. Perebeinos, V.; Rotkin, S. V.; Petrov, A. G.; Avouris, P. The Effects of Substrate Phonon Mode Scattering on Transport in Carbon Nanotubes. *Nano Lett.* **2009**, *9*, 312–316.
7. Li, Y.; Kinloch, I. A.; Windle, A. H. Direct Spinning of Carbon Nanotube Fibers from Chemical Vapor Deposition Synthesis. *Science* **2004**, *5668*, 276–278.
8. Koziol, K.; Vilatela, J.; Moisala, A.; Motta, M.; Cunniff, P.; Sennett, M.; Windle, A. High-Performance Carbon Nanotube Fiber. *Science* **2007**, *5858*, 1892–1895.
9. Stano, K.; Koziol, K.; Pick, M.; Motta, M.; Moisala, A.; Vilatela, J.; Frasier, S.; Windle, A. Direct Spinning of Carbon Nanotube Fibres from Liquid Feedstock. *Int. J. Mater. Form.* **2008**, *1*, 59–62.
10. Lu, J. P. Elastic Properties of Carbon Nanotubes and Nanoropes. *Phys. Rev. Lett.* **1997**, *79*, 1297–1300.
11. Yu, M.; Lourie, O.; Dyer, M. J.; Moloni, K.; Kelly, T. F.; Ruoff, R. S. Strength and Breaking Mechanism of Multiwalled Carbon Nanotubes under Tensile Load. *Science* **2000**, *5453*, 637–640.
12. Belytschko, T.; Xiao, S. P.; Schatz, G. C.; Ruoff, R. S. Atomistic Simulations of Nanotube Fracture. *Phys. Rev. B* **2002**, *65*, 235430.
13. Treacy, M. M. J.; Ebbesen, T. W.; Gibson, J. M. Exceptionally High Young's Modulus Observed for Individual Carbon Nanotubes. *Nature* **1996**, *381*, 678–680.
14. Ruoff, R. S.; Qian, D.; Liu, W. K. Mechanical Properties of Carbon Nanotubes: Theoretical Predictions and Experimental Measurements. *C.R. Phys.* **2003**, *4*, 993–1008.
15. Salvetat, J.; Briggs, G. A. D.; Bonard, J.; Bacsa, R. R.; Kulik, A. J.; Stöckli, T.; Burnham, N. A.; Forró, L. Elastic and Shear Moduli of Single-Walled Carbon Nanotube Ropes. *Phys. Rev. Lett.* **1999**, *82*, 944.
16. Zhang, X.; Li, Q. Enhancement of Friction between Carbon Nanotubes: An Efficient Strategy To Strengthen Fibers. *ACS Nano* **2010**, *4*, 312–316.
17. Vigolo, B.; Pénicaud, A.; Coulon, C.; Sauder, C.; Pailler, R.; Journet, C.; Bernier, P.; Poulin, P. Macroscopic Fibers and Ribbons of Oriented Carbon Nanotubes. *Science* **2000**, *5495*, 1331–1334.
18. Ericson, L. M.; Fan, H.; Peng, H.; Davis, V. A.; Zhou, W.; Sulpizio, J.; Wang, Y.; Booker, R.; Vavro, J.; Guthy, C.; *et al.* Macroscopic, Neat, Single-Walled Carbon Nanotube Fibers. *Science* **2004**, *5689*, 1447–1450.
19. Zhang, M.; Atkinson, K. R.; Baughman, R. H. Multifunctional Carbon Nanotube Yarns by Downsizing an Ancient Technology. *Science* **2004**, *5700*, 1358–1361.
20. Suzuki, T.; Ebert, R.-U.; Schüürmann, G. Development of Both Linear and Nonlinear Methods To Predict the Liquid Viscosity at 20 °C of Organic Compounds. *J. Chem. Inf. Comput. Sci.* **1997**, *37*, 1122–1128.

21. Pfeuffer, T.; Kürschner, K.; Strohriegl, P. Novel Nematic Bis-1,5-hexadiene Monomers: Synthesis and Photopolymerization to Cholesteric Polymer Networks. *Macromol. Chem. Phys.* **1999**, *11*, 2480–2486.
22. Sernetz, F.; Mülhaupt, R.; Waymouth, R. Homo-, Co- and Terpolymerization of 1,5-Hexadiene Using a Methylalumoxane Activated Mono-Cp-Amido-Complex. *Polym. Bull.* **1997**, *2*, 141–148.
23. Hall, A. W.; Lacey, D.; Buxton, P. I. The Use of Photoinitiated Free-Radical Cyclopolymerization in the Preparation of Novel Side-Chain Liquid-Crystalline Polydienes. *Macromol. Rapid Commun.* **1996**, *6*, 417–425.
24. Gokel, G. W. *Dean's Handbook of Organic Chemistry*, 2nd ed.; McGraw-Hill: New York, 2004.
25. Davies, R. J.; Riekel, C.; Koziol, K. K.; Vilatela, J. J.; Windle, A. H. Structural Studies on Carbon Nanotube Fibres by Synchrotron Radiation Microdiffraction and Microfluorescence. *J. Appl. Crystallogr.* **2009**, *42*, 1122–1128.
26. Li, J.; Kazakov, A.; Dryer, F. L. Experimental and Numerical Studies of Ethanol Decomposition Reactions. *J. Phys. Chem. A* **2004**, *38*, 7671–7680.
27. Stegner, G.; Balandin, A. A.; Rudenko, A. P. Mechanism of Carbon Formation in the Decomposition of Ethanol over a Copper—Silica Gel Catalyst. *Russ. Chem. Bull.* **1959**, *8*, 1811–1818.
28. Szymański, G. S.; Rychlicki, G.; Terzyk, A. P. Catalytic Conversion of Ethanol on Carbon Catalysts. *Carbon* **1994**, *2*, 265–271.
29. Esumi, K.; Ishigami, M.; Nakajima, A.; Sawada, K.; Honda, H. Chemical Treatment of Carbon Nanotubes. *Carbon* **1996**, *34*, 279–281.
30. Salzmann, C. G.; Llewellyn, S. A.; Tobias, G.; Ward, M. A. H.; Huh, Y.; Green, M. L. H. The Role of Carboxylated Carbonaceous Fragments in the Functionalization and Spectroscopy of a Single-Walled Carbon-Nanotube Material. *Adv. Mater.* **2007**, *19*, 883–887.
31. Karousis, N; Tagmatarchis, N.; Tasis, D. Current Progress on the Chemical Modification of Carbon Nanotubes. *Chem. Rev.* **2010**, *110*, 5366–5397.
32. Sarkar, S.; Bekyarova, E.; Niyogi, S.; Haddon, R. C. Diels—Alder Chemistry of Graphite and Graphene: Graphene as Diene and Dienophile. *J. Am. Chem. Soc.* **2011**, *133*, 3324–3327.